Arch. Metall. Mater. **67** (2022), 3, 1021-1026

DOI: https://doi.org/10.24425/amm.2022.139696

QIFENG TANG[1*], JINQING AO[1], BIYOU PENG[1], BIAO GUO[1], TAO YANG[1]

THERMODYNAMICS AND KINETICS ANALYSIS ON CARBOTHERMIC REDUCTION OF CALCINED MAGNESITE IN VACUUM

The carbothermic reduction of calcined magnesite in vacuum was studied. By thermodynamic analysis, the starting temperature of reduction reaction dropped from 2173K to 1523K when system pressure dropped from 1 atmosphere to 100 Pa. The experiments were carried out at different conditions under 10~100 Pa and the experimental results shown that the reduction extent of MgO improved by increasing the reaction temperature and time, the pellet forming pressure as well as adding fluoride as catalyst. The rate-determining step of carbothermic reduction process was gas diffusion with the apparent activation energy of 241.19~278.56 kJ/mol.

Keywords: calcined magnesite; carbothermic reduction; vacuum; thermodynamics; kinetics

1. Introduction

Metal magnesium is considered to be one of the most development and application potential green engineering materials in the 21st century due to its excellent performances such as low density, high specific strength, good chemical reactivity as well as great performances of electromagnetic shielding, noise reduction and shock absorption [1-3]. Therefore, magnesium is widely applied in various fields, such as metallurgy, chemistry, electronic technology, aviation, aerospace and automobile industry, etc.

There are two mainstream processes of magnesium production, namely, electrolysis of molten magnesium chloride and thermal reduction of magnesia [4]. Currently, the Pidgeon process is the dominant thermal reduction method in China and some other countries [5]. In Pidgeon process, MgO in calcined dolomite is reduced by ferrosilicon in a vacuum tube to produce magnesium and the reduction extent of MgO is relatively low, about 70%~80% [6]. In order to improve the MgO reduction efficiency and reduce the Mg production cost, the researcher developed other process, such as Balzano and Magnetherm processes. In Balzano process, raw materials are placed in a big size reduction tank and directly heated by the electric resistance, resulting in a large decrease in energy consumption [7]. Magnetherm process uses smelting reduction reaction in liquid slag to increase the reaction rate [8]. Si or SiFe alloy is used as a traditional reductant in above processess and is very expensive. If cheap carbon can be used as reductant, the costs of magnesium production will be significantly reduced, which will make carbothermic reduction process as one of the alternatives to the Pidgeon process [9-11].

In order to explore the feasibility of carbothermic reduction process for magnesium production, scholars have done a lot of research. For example, R. Winand carried out carbothermic reduction experiment at about 1700K for 5h in vacuum [12]. S. Zhong investigated the effects of vacuum pressure, reaction temperature and time on carbothermic reduction [13]. R.T. Li studied the catalytic effect of transition metals and found that the metals of Cu, Co, Ni and Fe could accelerate the carbothermic reaction rate [14]. In carbothermic reduction, the reaction between MgO and C belongs to solid-solid state reaction, the pellet forming pressure will affect the contact area between the reactants. Fluoride, as a common catalyst, is widely used in thermal reduction method [15]. In this work, we first determined the starting temperature of carbothermic reduction by thermodynamic calculations, and then carried out the experiments of carbothermic reduction of calcined magnesite under vacuum. The effects of reaction temperature, pellet forming pressure and fluoride catalysts on the MgO reduction extent were investigated. Finally, the kinetic characteristics of carbothermic reduction of MgO were obtained by comparing the linear fitting curves with the apparent activation energy. The results shown that MgO in calcined magnesite could be effectively reduced by graphite and the reduction extent was as high as nearly 90% in this experiment.

[1] XIHUA UNIVERSITY, COLLEGE OF MATERIALS SCIENCE AND ENGINEERING, CHENGDU 610039, PR CHINA

* Corresponding author: tqfkmust@126.com

2. Reaction thermodynamic

In the process of carbothermic reduction of calcined magnesite, magnesium oxide reacts with carbon to generate magnesium and carbon monoxide vapors. Under atmosphere, the chemical reaction and thermodynamic equation could be expressed as follows [16,17]:

$$MgO_{(s)} + C_{(s)} = Mg_{(g)} + CO_{(g)}$$
$$\Delta G^{\Theta} = 647929 + 30.84T\lg T - 404.43T \quad (1)$$

where ΔG^{Θ} stands for the Gibbs standard free energy, and T is the reaction temperature. By calculating Eq. (1), the relationship between the Gibbs standard free energy of reaction and temperature was listed in TABLE 1. It can be concluded that the Gibbs standard free energy decreases as the temperature rises. When reaction temperature reach 2073K and 2173K, the Gibbs standard free energy are calculated to be 21.6 kJ and –7.2 kJ, respectively. These also mean that the starting temperature of carbothermic reduction reaction at atmosphere pressure must be higher than 2173K.

Under atmosphere, in addition to the starting temperature of carbothermic reduction is too high, the magnesium vapor extracted from magnesite is also easy to be re-oxidized by oxygen in the air. In order to avoid the deficiencies mentioned above, carbothermic reduction reaction should be carried out in vacuum, where the Gibbs actual free energy ΔG could be described by the Eq. (2):

$$\Delta G = \Delta G^{\Theta} + RT\ln K \quad (2)$$

where R is the gas constant, and K denotes reaction equilibrium constant which is defined as below:

$$K = [(P_{Mg}/P_0)*(P_{CO}/P_0)]/(a_{MgO}*a_C) \quad (3)$$

where P_0, P_{Mg} and P_{CO} represent atmospheric pressure, Mg vpour pressure, CO gas pressure, a_{MgO} and a_C are activity of MgO and C, respectively. Because MgO and C are solid state in the reaction, both the values of a_{MgO} and a_{CO} are equal to 1. Thus, the equilibrium constant K is only related to Mg vapor and CO gas. Under vacuum condition, the system pressure P_s is the sum of P_{Mg} and P_{CO}.

Combining above equations, the Gibbs actual free energy of carbothermic reduction reaction in vacuum could be expressed by the Eq. (4):

$$\Delta G = \Delta G^{\Theta} + RT\ln(P_s/2P_0)^2 = 647929 +$$
$$+ 30.84T\lg T - 404.43T + 16.628T[\ln(P_s/P_0) - \ln 2] \quad (4)$$

Fig. 1 displays the Gibbs actual free energy trend of carbothermic reduction reaction at different system pressure and temperature. As shown in Fig. 1, the use of vacuum, accelerating Mg vapor diffusion, can significantly reduce the starting temperature of reaction. The starting temperature decreases from 2173K to 1523K when the system pressure drop from 1atm to 100 Pa. Further reduce the system pressure to 10 Pa, the starting temperature would be lower than 1373K.

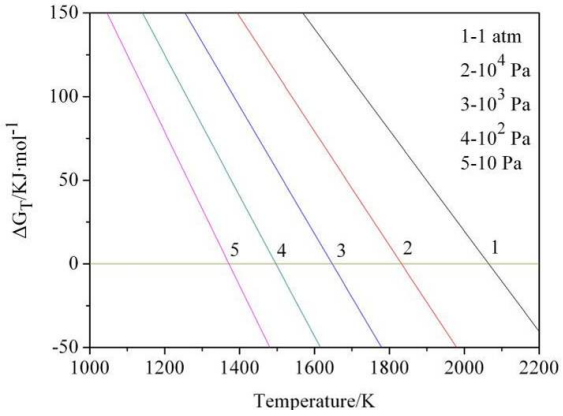

Fig. 1. Gibbs free energy of carbothermic reduction at different pressures and temperatures

3. Experimental

Based on the thermodynamic calculations, the experiments of carbothermic reduction were carried out. Calcined magnesite (98% MgO) powder was supplied by the Chongqing Haibo magnesium smelting Co., Ltd, and graphite (99.85% C) powder was used as reductant. Catalyst powder (CaF_2 and MgF_2) purity was greater than 99%. All powders were passed through the -240 mesh sieve.

In order to ensure sufficient amount of reducing agent, calcined magnesite and graphite were weighed in a molar ratio (MgO/C = 1/3). The raw materials were mixed thoroughly, and compacted into 10mm-diameter and 30 mm-height pellets. About 150 g pellets placed in graphite crucible, and then transferred into the high-temperature vacuum furnace which was internally heated by using a regulated graphite resistance and had a maximum temperature of 1873K. The reduction process was controlled under 10~100 Pa, and the actual experimental reaction temperatures were higher than the calculated values for improving the reaction rate. After reduction, the residue pellets in graphite crucible was cooled to room temperature for subsequent measurements. The reduction extent of MgO (α) in pellets was calculated by the follow equation:

$$\alpha = (W_0 - W_t)/W_0 \times 100\% \quad (5)$$

where W_0 and W_t represent the weights of MgO before and after reaction, respectively.

TABLE 1

Gibbs standard free energy of reaction at different temperature under atmosphere

Temperature/K	1573	1673	1773	1873	1973	2073	2173	2273	2373	2473
ΔG^{Θ}/kJ·mol^{-1}	166.8	137.6	108.5	79.5	50.5	21.6	–7.2	–35.8	–65.8	–93.4

4. Results and discussion

4.1. Effect of reaction temperature and time

In this work, we chose three experimental temperatures, 1673K, 1723K and 1773K, respectively, and the reaction times in the range of 15-120 min. The compacting pressure of pellets was 60 MPa and there was no fluoride catalyst in primary pellets. The dependence of the reduction extent of MgO on different temperature are presented in Fig. 2. It could be seen that the reduction extent increased with increasing of reaction temperature as well as extending of reaction time. At relatively low temperature and short time, the reduction extent was only about 18% at 1673K for 15 min. When the temperature reached 1773K and the time was extend to 120 min, the reduction extent was as high as approximately 85%, which is slightly higher than that of the silicothermic process.

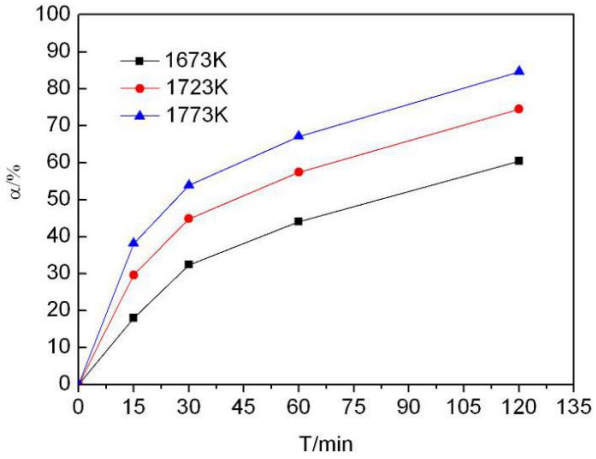

Fig. 2. Effect of reaction temperature and time on the reduction extent of MgO

Fig. 3 shows the macro morphologies of residue at different reduction extent of MgO. The pellets were in good shape with some slight holes on the surface at lower reduction extent. As the reduction extent increased, calcined magnesite and graphite in pellets were consumed constantly by reduction reaction, which caused more holes on the surface of pellets with the dropping of pellet strength. The pellets became extremely loose and eventually collapsed when the reduction extent was very high. The residue pellets at different reduction extent were checked by XRD and the results were presented in Fig. 4. The XRD patterns confirmed that MgO and C were main phases in pellets and the intensity of MgO phase in residue pellets weakened as the reduction extent increased.

4.2. Effect of pellet forming pressure

Taking into account of energy consumption and reaction rate, we chose a compromise temperature, namely, 1723K, to investigate the effect of pellet forming pressure on the reduction

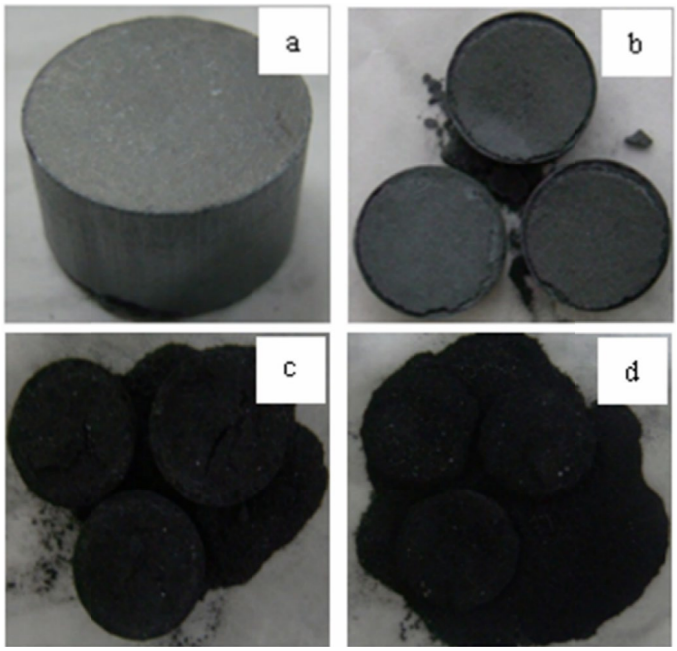

Fig. 3. Macro morphologies of residue at different reduction extent of MgO: (a) Primary pellet, $\alpha = 0$; (b) $\alpha = 18\%$; (c) $\alpha = 45\%$; (d) $\alpha = 85\%$

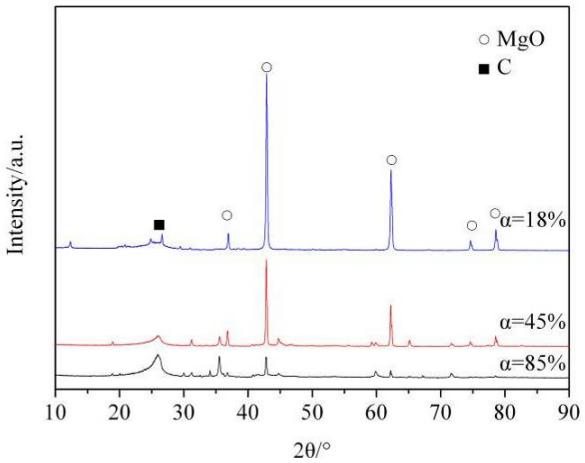

Fig. 4. XRD patterns of residue at different reduction extent of MgO

extent of MgO. The trends of MgO reduction extent at different forming pressure are shown in Fig. 5. The reduction extent increased as the pellet forming pressure increased. The reduction extent improved evidently from 62.1% to 74.5% at 1723K for 120 min when the pellet forming pressure was raised from 30 MPa to 60 MPa. This is because, at lower pressure, the reaction contact area between calcined magnesite and graphite was getting larger by increasing the pellet forming pressure. Further increasing the pellet forming pressure, the growth of reduction extent was slow down. The final reduction extent reached 78.2% and 80.3% at 90 MPa and 120 MPa, respectively. In this case, when the forming pressure exceeded a certain critical value, the gas diffusion channel reduced due to the increase of pellet density, which eventually led to that the escape of the produced magnesium vapor was hindered. Base on the results of the experiments, the optimal pellet forming pressure was 60 MPa.

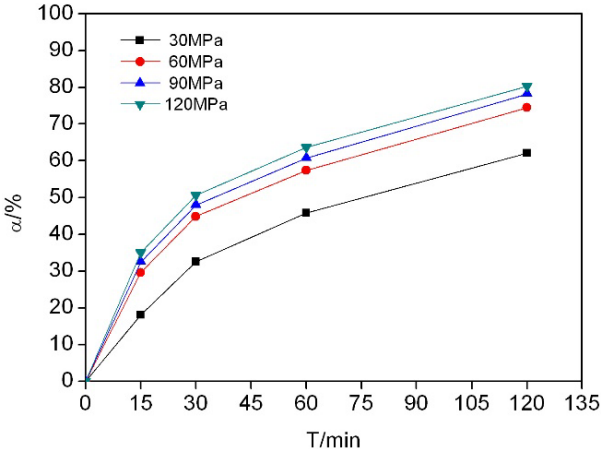

Fig. 5. Effect of pellet forming pressure on the reduction extent of MgO

4.3. Effect of fluoride

In the process of magnesium production by thermal reduction reaction, MgF_2 and CaF_2 are common additives as catalyst and could greatly improve the reduction extent of MgO [18]. In order to assess the effect of catalyst species on the reduction extent, we added 3% fluoride as catalyst into the primary pellets. The experiments were carried out with the reaction temperature of 1723K and the pellet forming pressure of 60 MPa, and the results are displayed in Fig. 6. The results suggests that the reduction extent of the primary pellets containing fluorides were higher than that of those without additives, and CaF_2 had a slightly better catalytic effect than MgF_2. Adding fluoride could improve the activity of MgO by increasing surface reaction energy and accelerate the mass transfer rate by forming low melting point slag [19]. The MgO reduction extent of primary pellets with 3% CaF_2 and with 3%MgF_2 were 87.3% and 85% at 120 min, respectively.

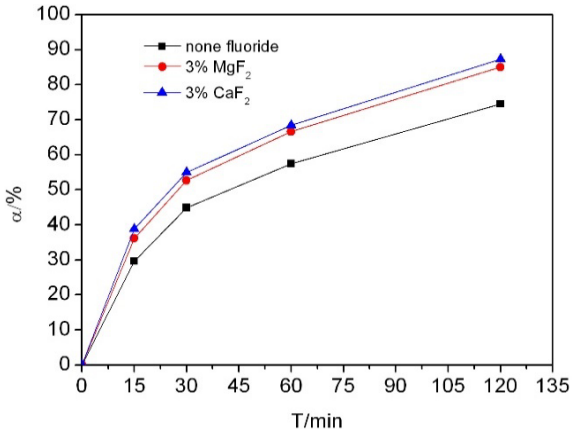

Fig. 6. Effect of fluoride on the reduction extent of MgO

5. Reaction kinetic

In vacuum, the proceding of carbothermic reduction reaction of magnesia at high temperature are influenced by many factors such as temperature, system pressure, particle size and reaction products. The kinetics model of carbothermic reduction is a shrinking core model [20-22], which could be summarized as follows:

(1) Carbon gasifies and then towards the surface of MgO;
(2) Reaction takes place on the MgO/C interface;
(3) Mg vapor and CO gas leave the reaction interface and diffuse through the residue pellets.

The reduction reaction rate of MgO is mainly affected by the above mentioned procedures. Therefore, there are three kinetic models in carbothermic reduction process, namely, carbon gasifition, interface reaction and gas diffusion, respectively. In this work, the molar ratio of C/Mg in primary pellets is 3. When carbothermic reduction is controlled by carbon gasifition, interface reaction or gas diffusion, the dependencies of the reaction rate a on the reaction time t could be represented by the follow formulas [23,24].

1. Carbon gasifition:

$$\ln(1 - a/3) = -kt \tag{6}$$

2. Interface reaction:

$$1 - (1 - a/3)^{1/3} = \ldots kt \tag{7}$$

3. Gas diffusion:

$$[1 - (1 - a/3)^{1/3}]^2 = -kt \tag{8}$$

$$1 - 2a/3 - (1 - a)^{2/3} = -kt \tag{9}$$

where k is known as the apparent rate constant. Based on experimental results, the relationship between a and t in different kinetic models are linearly fitted. The results are illustrated in Fig. 7(a-d) and listed in TABLE 2.

TABLE 2

Value of apparent rate constant k and Adj. R-square (r) of fitting line at different condition

Temperature/K	Carbon gasification			Interface reaction		
	r	r_A	k	r	r_A	k
1673	0.91073		0.00214	0.94209		0.00246
1723	0.85809	0.865	0.00279	0.91965	0.927	0.00344
1773	0.8247		0.00329	0.91866		0.00436
Temperature/K	**Gas diffusion 1**			**Gas diffusion 2**		
	r	r_A	k	r	r_A	k
1673	0.99398		0.00057	0.99667		0.00047
1723	0.99754	0.996	0.00109	0.99819	0.997	0.00085
1773	0.99667		0.00175	0.99779		0.00126

*: r_A stands for the average of Adj. R-square (r).

It is can be seen that the linear relationship performed the best in Fig. 7(c-d). The Adj. R-square (r) of fitting in Fig. 7(c-d) were in the range from 0.994 to 0.998 with an average value of 0.997, which reveals that the process of carbothermic reduction in vacuum is mainly dominated by gas diffusion.

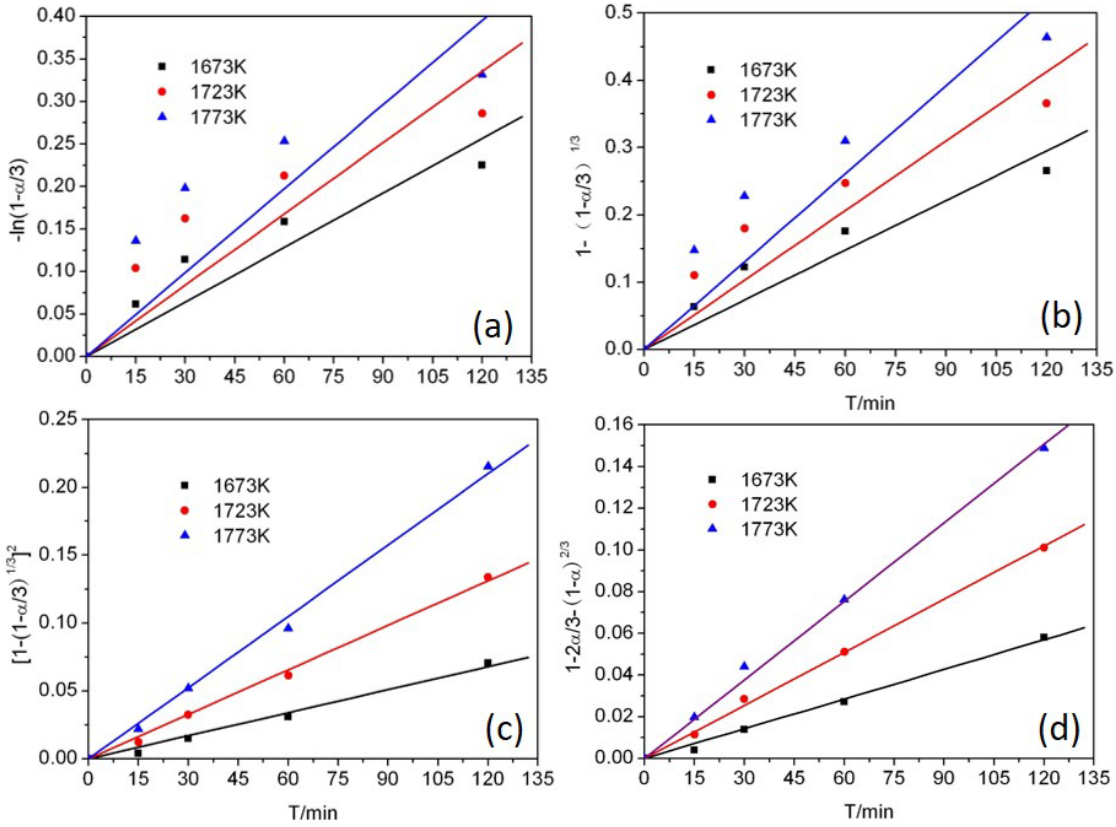

Fig. 7. The relationship between a and t in different kinetic models: (a) Carbon gasifition; (b) Interface reaction; (c) and (d) Gas diffusion

The relationship between apparent rate constant k and reaction temperature T could be expressed by Arrhenius equation as follows:

$$k = A\exp\left(-\frac{E}{RT}\right) \tag{10}$$

where A represents frequency factor, E stands for apparent activation energy, R is gas constant, respectively. Logarithming of Eq. (10) gave:

$$\ln k = -\frac{E}{R}\frac{1}{T} + \ln A \tag{11}$$

The dependencies of ln$k$ on T^{-1} at 1673K, 1723K and 1773K are shown in Fig. 8. The regression equations of ln$k$ vs. T^{-1} and the apparent activation energy values are determined from slopes of the straight lines and listed in TABLE 3. The values of the apparent activation energy in two kinetic models of gas diffusion were calculated to be 241.19 kJ·mol^{-1} and 278.56 kJ·mol^{-1}, respectively, higher than the values in the other two cases, indicating that the effect of gas diffusion was greater than that of carbon gasifition and interface reaction, in agreement with the results of literature [25,26]. Therefore, gas diffusion is

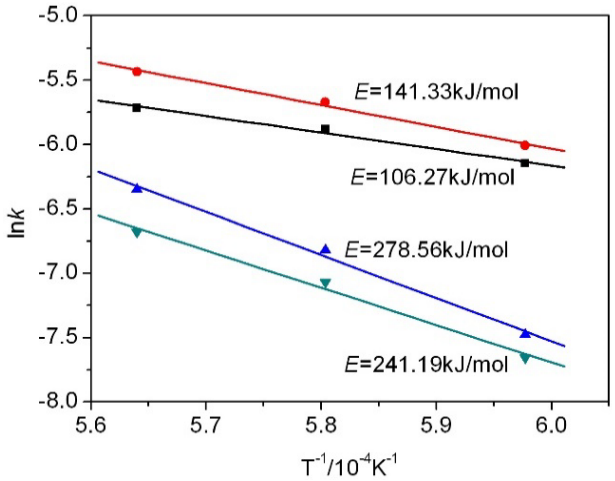

Fig. 8. The dependences of ln$k$ on 1/T at 1673~1773K

TABLE 3

Apparent activation energy with different assumed mechanisms

Rate controlling step	Rate equation	Regrssion equation of ln$k$ vs. T^{-1}	E (kJ mol^{-1})
Carbon gasification	$-\ln(1-a/3) = kt$	$\ln k = 1.50769-12781.4T^{-1}$	106.27
Suface reaction	$1-(1-a)^{1/3} = kt$	$\ln k = 4.1667-16999.5T^{-1}$	141.33
Gas difuusion 1	$[1-(1-a)^{1/3}]^2 = kt$	$\ln k = 12.57468-33505T^{-1}$	278.56
Gas difuusion 2	$1-2a/3-(1-a)^{2/3} = kt$	$\ln k = 9.71334-29011.1T^{-1}$	241.19

the rate-determining step in the process of carbothermic reduction of calcained magnesite in vacuum.

6. Conclusions

Calcained magnesite was reduced by graphite in vacuum. The following results were obtained:

1. By thermodynamic analysis, the Gibbs free energies for reaction between magnesia and carbon were calculated as a function of temperature and pressure. The starting reaction temperature of carbothermic reduction of magnesia reached 2173K under atmosphere; The use of vacuum could effectively reduce the starting temperature, which decreased to about 1523K and 1373K when the system pressure dropped to 100 Pa and 10 Pa, respectively.
2. The experiments of carbothermic reduction of calcined magnesite were carried out at 120 min under 10~100 Pa. The reduction extent of MgO increased by increasing the reaction temperature and the pellet forming pressure as well as adding fluorides as catalysts. Under optimized process parameters, the MgO reduction efficiency reached up to the maximum value with 87.3%.
3. Based on the experimental results at temperature of between 1673K and 1773K, the effect of gas diffusion on carbothermic reduction was greater than that of carbon gasifition and interface reaction. Gas diffusion was the rate-determining step of reduction process, in which the apparent activation energy was estimated to be 241.19~278.56 $kJ \cdot mol^{-1}$.

Acknowledgements

This work was financially supported by Key Scientific Research Fund of Xihua University (Grant No. Z1320109) and Sichuan Province Department of Science and Technology Fund for Nature (Grant No. 19ZDYF2931(2019YFG70511)).

REFERENCES

[1] B.L. Mordike, T. Ebert, Mater. Sci. Eng. A **302**, 37 (2001).
[2] D. Eliezer, E. Aghion, F.H. Froes, Adv. Perform. Mater. **5**, 201 (1998).
[3] H. Friedrich, S. Schumann, J. Mate. Proces. Tech. **117**, 276 (2001).
[4] S. Ramakrishnan, P. Koltun, Resour. Conservat. Recycl. **42**, 49(2004).
[5] F. Gao, Z.R. Nie, Z.H. Wang, et al., Int. J. Life Cycle Assess. **14**, 480 (2009).
[6] W.Y. Liang, X.L. Sun, F.S. Li, et al., China Nonferrous Metallurgy **4**, 36 (2020).
[7] F.D'Errico, G. Perricone, R. Oppio, JOM **61**, 14 (2009).
[8] D. Minic, D. Manasijevic, J. Dokic, et al., J. Therm. Anal. Calorim. **93**, 411 (2008).
[9] G. Brooks, S. Trang, P. Witt, et al., JOM **58**, 51 (2006).
[10] Y. Takeshi, M. Kazuki. Mater. Trans. **44**, 722 (2003).
[11] I. Vishnevetsky, M. Epstein, Solar Energy **111**, 236 (2015).
[12] R. Winand, M.V. Gysel, A. Fontana, et a.l, Trans. Inst. Min. Metall. C **99**, 105 (1990).
[13] Z.H. Li, H.S. Xiang, Y.N. Dai, Energy for Metallurgical Industry **23**, 20 (2004).
[14] R.T. Li, W. Pan, S. Masamichi Sano et al., Thermochim. Acta **398**, 265 (2003).
[15] Y. Tian, T. Qu, B. Yang, et al., Metall. Mater. Trans. B **43**, 657(2012).
[16] N. Yoshikawa, E. Ishizuka, K. Mashiko, et al., Mater. Lett. **61**, 2096 (2006).
[17] Q.F. Tang, J.C. Gao, X.H. Chen, et al., Mater. Rev. **28**, 64 (2016).
[18] Y. Tian, T. Qu, B. Yang, et al., Metal. Mater. Trans. B **43**, 657 (2012).
[19] Y. Jiang, Y.Q. Liu, H.W. Ma, et al., Metal. Mater. Trans. B **47** 873 (2016).
[20] W. Gruner, S. Stolle, L.M. Berger, et al., Int. J. Refractory Met. Hard Mater. **17**, 227 (1999).
[21] V.L. Boris, L.U. Valery, Thermochim. Acta **401**, 139 (2002).
[22] A. Sondhi, C. Morandi, R.F. Reidy, Ceram. Int. **39**, 4489 (2012).
[23] E. Busenberg, L.N. Plummer, Am. J. Sci. **282**, 45 (1982).
[24] M.C. Abraham, A. Ghosh, Ironmak. Steelmak. **6**, 14 (1979).
[25] R.T. Li, W. Pan, S. Masamichi, et al., Thermochim. Acta **395**, 145 (2002).
[26] W.D. Xie, J. Chen, H. Wang, et al., Rare Met. **35**, 192 (2016).